SANDWICHED VIDEO COMPRESSION: EFFICIENTLY EXTENDING THE REACH OF STANDARD CODECS WITH NEURAL WRAPPERS

Berivan Isik [*] *, Onur G. Guleryuz* [†]*, Danhang Tang* [†]*, Jonathan Taylor* [†]*, and Philip A. Chou* [†]

[*]Stanford University, [†]Google Research
`berivan.isik@stanford.edu,`
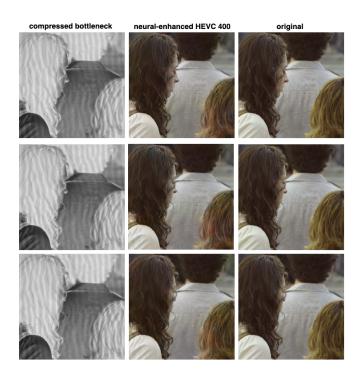`{oguleryuz,danhangtang,jontaylor,philchou}@google.com`

ABSTRACT

We propose sandwiched video compression – a video compression system that wraps neural networks around a standard video codec. The sandwich framework consists of a neural pre- and post-processor with a standard video codec between them. The networks are trained jointly to optimize a rate-distortion loss function with the goal of significantly improving over the standard codec in various compression scenarios. End-to-end training in this setting requires a differentiable proxy for the standard video codec, which incorporates temporal processing with motion compensation, inter/intra mode decisions, and in-loop filtering. We propose differentiable approximations to key video codec components and demonstrate that the neural codes of the sandwich lead to significantly better rate-distortion performance compared to compressing the original frames of the input video in two important scenarios. When transporting high-resolution video via low-resolution HEVC, the sandwich system obtains 6.5 dB improvements over standard HEVC. More importantly, using the well-known perceptual similarity metric, LPIPS, we observe 30% improvements in rate at the same quality over HEVC. Last but not least we show that pre- and post-processors formed by very modestly-parameterized, light-weight networks can closely approximate these results.

1. INTRODUCTION

The last decade has witnessed neural image compression methods [1] gradually outperforming traditional image compressors such as JPEG2000 and HEIC [2] and replacing them as state-of-the-art image compressors. The success of neural image compressors is due to their ability to perform complex non-linear transforms, which are learned end-to-end through back-propagation [3]. More recently, the first learned video compressors have been proposed [4] and research on improving neural video compressors has accelerated [5, 6, 7, 8]. The existing strategies focus mainly on learning how to predict flows, warp the previous reconstructions with the predicted flows, and do residual compensation, all with neural networks trained end-to-end. This has lead to very complex networks with tens of millions of parameters [6, 7], tens of millions of floating point operations per pixel, and weeks of training on high end GPUs [9].

In this work, we propose a computationally more efficient way of improving upon any standard video codec by using neural networks. In particular, we sandwich a standard video codec between lightweight neural pre- and post-processors, and optimize them end-to-end. Our approach leverages existing highly optimized computational implementations of the standard codec and the seamless network-transport of standard bit-streams over network nodes already familiar with such traffic. The proposed neural pre- and post-processors learn how to perform non-linear transformations on the

---

Work done while the first author was an intern at Google.

Fig. 1. Toy example with gray-scale codec (HEVC4:0:0). The sandwich is used to transport full color video over a codec that can only transport gray-scale. Frames of neural codes decoded by the standard codec (compressed bottlenecks), final reconstructions by the post-processor, and original source videos, at time t, $t+1$, and $t+2$ are shown. Rate=0.50 bpp, PSNR=39.3dB, fps=30. Note that the sandwich establishes temporally consistent modulation-like patterns on the bottlenecks through which the pre-processor encodes color that is then demodulated by the post-processor for a full-color result.

input and the output of the standard codec for the best rate-distortion performance while the standard video codec does the heavy lifting by performing the usual video coding operations on the output of the neural pre-processor. Our work is primarily geared toward adapting the standard codec to compression scenarios that are outside the immediate scope of its design. In so doing we are interested not only in significant improvements but also in understanding how the neural networks accomplish those improvements. As the networks have to generate viewable 8-bit video that is related to the original visual scenes, it is typically possible to observe their operation even if at a coarse level (see for instance the toy example of Figure 1).

Figure 2 summarizes our approach. For the ith video clip with frames $t = 0, 1, 2, \ldots$, source images $\{I_i(t)\}$ are processed by a
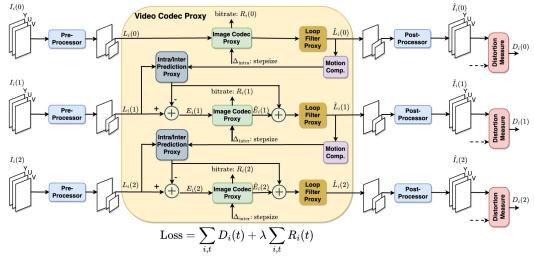
Fig. 2. Sandwich architecture during training. The shaded box (video codec proxy) is replaced with a standard video codec at inference.

neural pre-processor in a temporally independent fashion to obtain "bottleneck" images $\{L_i(t)\}$. The bottleneck images contain neural latent codes representing the source images, but are nevertheless in 4:4:4 (or 4:2:0) format ready for compression by the standard video codec. The standard video codec compresses the bottleneck images into reconstructed bottleneck images $\{\hat{L}_i(t)\}$, again in 4:4:4 format. Finally, the reconstructed bottleneck images are processed by a neural post-processor into reconstructed source images $\{\hat{I}_i(t)\}$. To train the neural pre- and post-processors, we replace the standard video codec by a differentiable proxy (shown shaded in yellow) and we minimize the total rate-distortion Lagrangian $\sum_{i,t} D_i(t) + \lambda R_i(t)$, where $D_i(t)$ and $R_i(t)$ are the distortion and rate of frame t in clip i. At evaluation, the standard video codec is used instead of the proxy.

Our framework is inspired by previous work on sandwiched image compression [10, 11], which shares the motivation to improve over standard codecs in rate-distortion performance, while leveraging their implementation-related conveniences. The end-to-end learned image codecs that outperform the standard image codecs in rate-distortion performance [1, 12, 13, 14] require over-parameterized networks and entropy models, which have significant time, power, and resource costs. [10, 11] proposed a solution to this by wrapping neural networks around a standard image codec. Training the sandwich end-to-end requires a differentiable proxy for the standard image codec. The authors trained the sandwiched model by replacing the standard image codec with a differentiable JPEG proxy that uses 8×8 DCTs and straight-through quantization[1] as a proxy for the quantization step, and a differentiable function as an approximation of the bit rate from the entropy coding step. They showed that with training, the pre-processor and post-processor would learn to communicate with each other by sending neural codes in the form of spatial modulation patterns that represent details of the original input. The patterns are easy to compress with a standard codec while being robust to its degradations. Gains over the standard codec alone were shown to be especially noteworthy when the input has different characteristics than intended for the standard codec. In particular, [10] showed high gains when coding multispectral or normal map images, while [11] showed high gains when coding high dynamic range or high resolution images with a LDR or LR codec.

Our motivation and approach are similar to [10, 11] but in this paper we make the fundamental leap of transferring the sandwich

approach from images to video. This leap is challenging for a number of reasons. First, independently pre- and post-processing the video frames may be problematic, as the neural codes in the bottleneck images need to be temporally coherent in order for the video codec to take advantage of motion compensation. It is not at all clear that modulation-like high frequency patterns will be well-represented through motion compensation. Second, standard video codecs [15]–[20] are substantially more complicated than image codecs, involving not only motion estimation and compensation, but also mode selection, loop filtering, and many other aspects. In this paper, we address these issues, while showing results for sandwiched video compression that parallel the earlier results for sandwiched image compression, including multispectral (color video compressed by grayscale video codecs) and super-resolution (high resolution video compressed by standard resolution video codecs) applications. Moreover, we get gains over standard codecs with networks on the order of 100K parameters (pre and post combined), a reduction in complexity by two orders of magnitude over state-of-the-art neural video compressors. Few works prior to ours sandwich a standard video codec between neural processors. Those that do, e.g. [21, 22, 23], do so in such a way that the pre- and post-processors may be used independently — thus do not take full advantage of the communication available between pre- and post-processors. Our contributions can be summarized as:

(1) We propose a sandwiched video compression framework that provides more efficient training and inference due to the simplicity of the neural networks but still enjoys the flexibility of neural networks in learning non-linear transforms.

(2) We propose a differentiable video codec proxy that can be used effectively in the training loop.

(3) We demonstrate that the sandwiched HEVC obtains 6.5 dB improvement over the standard HEVC 4:4:4 in low-resolution transport (8 dB improvement over 4:0:0 when coding color over gray-scale.) Moreover, when optimized for and tested with a perceptual similarity metric, Learned Perceptual Image Patch Similarity (LPIPS), we observe $\sim 30\%$ improvements in rate at the same quality over the standard HEVC 4:4:4.

2. METHOD

2.1. Video Codec Proxy

Our video codec proxy, shown in Figure 2, maps an input group of images (like a group of pictures, or GOP) to an output group of images, plus a bit rate for each image. The details of our video codec proxy can be summarized as follows.

---

[1]A straight-through quantizer is a software-implemented function $y = Q(x)$ that implements ordinary quantization in the forward direction but pretends to have a gradient dy/dx of 1 instead of 0 in the backward direction.

Intra-Frame Coding. The video codec proxy simulates coding the first ($t = 0$) frame of the group, or the I-frame, using the image codec proxy from [10, 11].

Motion Compensation. The video codec proxy simulates predicting each subsequent ($t > 0$) frame of the group, or P-frame, by motion-compensating the previous frame, whether the previous frame is an I-frame or a P-frame. Motion compensation is performed using a "ground truth" dense motion flow field obtained by running a state-of-the-art optical flow estimator, UFlow [24], between the original source images $I_i(t)$ and $I_i(t-1)$. The video proxy simply *applies* this ground truth motion flow to the previous reconstructed bottleneck image $\hat{L}_i(t-1)$ to obtain an inter-frame prediction $\tilde{L}_i(t)$ for bottleneck image $L_i(t)$. This simulates motion compensation in a standard codec operating on the bottleneck images. Note that our motion compensation proxy does not actually depend on $L_i(t)$, so although it is a warping, it is a linear map from $\hat{L}_i(t-1)$ to $\tilde{L}_i(t)$, with a constant Jacobian. This makes optimization much easier than if we had tried to use a differentiable function of both $\hat{L}_i(t-1)$ and $L_i(t)$, like UFlow itself, that *finds* as well as *applies* a warping from $\hat{L}_i(t-1)$ to $L_i(t)$. Such functions have notoriously fluctuating Jacobians that make training difficult.

Prediction Mode Selection. Our video codec proxy also simulates Inter/Intra prediction mode decisions. This ensures better handling of temporally occluded/uncovered regions in video. First, Intra-prediction is simulated by rudimentarily compressing the current-frame and low pass filtering it. This simulates filtering, albeit not the usual directional filtering, to predict each block from its neighboring blocks. Initial rudimentary compression ensures that the intra-prediction proxy is not unduly preferred at very low rates. For each block, the Intra prediction (from spatial filtering) is compared to the Inter prediction (from motion compensation), and the one closest to the input block determines the mode of the prediction.
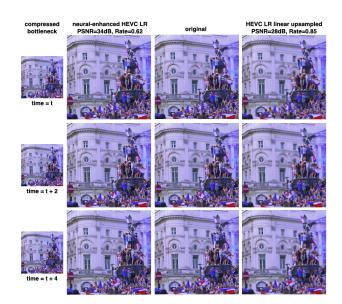
Residual Coding. The predicted image, comprising a combination of Intra- and Inter-predicted blocks, is subtracted from the bottleneck image, to form a prediction residual. The residual image is then compressed using the image codec proxy of [10, 11]. The compressed residual is added back to the prediction to obtain a "pre-filtered" reconstruction of the bottleneck image $\hat{L}_i(t)$.

Loop Filtering. The "pre-filtered" reconstruction is then filtered by a loop filter to obtain the final reconstructed bottleneck image $\hat{L}_i(t)$. The loop filter is implemented with a small U-Net((8);(8, 8)) [25] that processes one channel at a time. The loop filter is trained once for four rate points on natural video using only the video codec proxy with rate-distortion (ℓ_2) training loss in order to mimic common loop filters. The resulting tandem of filters are kept fixed for all of our simulations, i.e., once independently trained, the loop filters for four rate points are not further trained.

Rate Proxy. Similar to [10, 11] the differentiable rate for each frame is obtained as $R(E_i(j)) = a \sum_{k,l} \log(1 + |e_l^{(k)}|/\Delta)$, where $e_l^{(k)}$ is the lth coefficient of the kth block of DCT coefficients, and a is chosen such that $R(E_i(j))$ is the actual rate at which JPEG codes $E_i(j)$ with uniform stepsize Δ. An alternative proxy is given in [26].

2.2. Pre- and Post-Processors

The pre- and post-processors are implemented as a 1×1 conv-network (a multilayer perceptron acting pixelwise) in parallel with a U-Net. The intuition is that the 1×1 conv-network learns the appropriate color space conversion and tone mapping, while U-Net adds or removes spatial modulation patterns, or watermarks, which serve as the neural codes. We report results with U-Nets of two different complexities. As U-Net encoder/decoder filters, the high complexity network

Fig. 3. Sandwich of HEVC LR: Frames from compressed bottlenecks, reconstructions by sandwich, original source videos, and HEVC LR. Note the substantially improved definition on the crowd and the building. While not shown here the sandwich system also obtains significant improvements over neural-post-processed HEVC LR thanks to the information embedded by the neural pre-processor.

uses U-Net((32, 64, 128, 256); (512, 256, 128, 64, 32)) ($\sim$ 8M parameters). Our low complexity, *slim* network uses U-Net((32); (32, 32)) ($\sim$ 57 thousand parameters), with a $\sim$ **99%** reduction in parameters.

2.3. Loss Function

As mentioned in the Introduction, the pre- and post-processors, and the loop filter in the video codec proxy, are trained to minimize the total rate-distortion Lagrangian $\sum_{i,t} D_i(t) + \lambda R_i(t)$, where $D_i(t)$ and $R_i(t)$ are the distortion and rate of frame t in clip i. The rate term in particular serves to encourage the pre- and post-processors to produce temporally consistent neural codes, since neural codes that move according to our "ground truth" motion flow field will be well predicted, leading to smaller residuals and rate terms. We do indeed observe that the resulting neural codes seem to have some degree of temporal consistency, as shown in Figure 1. Note that the overall mapping from the input images through the pre-processor, video codec proxy, post-processor, and loss function is differentiable.

3. EXPERIMENTS

3.1. Setup and Dataset Specifications

We generated a video dataset that consists of 10-frame clips of videos from the AV2 Common Test Conditions [27] and their associated motion flows, calculated using UFlow [24]. We used a batch size of 8, i.e., 8 video clips in each batch. Each clip is processed during the dataset generation step such that it has 10 frames of size 256x256, selected from video of fps 20-40. HEVC is implemented using x265 (IPP.., single reference frame, rdoq and loop filter on.). We compare the sandwich model with the standard codec, HEVC, under three settings: (1) YUV 4:0:0 format with single-channel (grayscale) bottlenecks in Figure 4, (2) YUV 4:4:4 format in low-resolution (LR) bottlenecks in Figure 5, and (3) YUV 4:4:4 format using the Learned Perceptual Image Patch Similarity (LPIPS) – a common perceptual similarity metric in the literature [28]. In each setting, the model is trained for 1000 epochs, with a learning rate 1e-4, and tested on

120 test video clips. All R-D plots are over the entire test set. We report results in terms of YUV PSNR when using the ℓ_2 norm and "LPIPS (RGB) PSNR" when using LPIPS. Because LPIPS is intended for RGB, for the latter the final decoded YUV video is converted into RGB and then LPIPS computed. In order to report results on an approximately similar scale we derived a fixed linear scaler for LPIPS so that for image vectors x, y,

$$sLPIPS(x, y) \sim ||x - y||^2, \text{if } ||x - y||^2 < \tau \qquad (1)$$

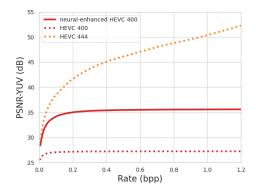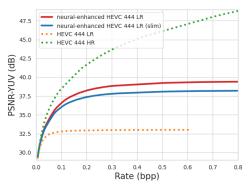where τ is a small threshold and s is the LPIPS linear scaler.

Fig. 4. RD performance of the YUV 4:0:0 sandwich.

3.2. Results

YUV 4:0:0. Figures 1 and 4 show the subjective and quantitative results with sandwiched HEVC YUV 4:0:0 codec. As can be seen from the bottleneck frames in Figure 1, sandwich model is able to preserve the temporal consistency between the frames, which enables the standard codec HEVC to take advantage of the modulation patterns to achieve a better rate-distortion point. Quantitatively, Figure 4 shows the substantial improvements (by 8 dB) of the sandwich model over HEVC YUV400.

Fig. 5. RD performance of YUV 4:4:4 low-resolution (LR) sandwich. (HEVC 444 HR stands for HEVC YUV 4:4:4 high-resolution.)

Low-Resolution (LR). Figures 3 and 5 show the subjective and quantitative results with sandwiched HEVC YUV 4:4:4 LR codec. The standard LR codec transports LR video that is a linearly downsampled (bicubic) version of the original. Decoded video is linearly upsampled (lanczos3). In the case of the sandwich, the exact same system is used but with generated bottlenecks. The 6.5 dB improvement of the sandwich model with HEVC YUV 4:4:4 LR over the standard HEVC YUV 4:4:4 LR in Figure 5 is also visible in the subjective comparison provided in Figure 3 which demonstrates the

Fig. 6. HEVC with LPIPS: Inter-frames from reconstructions by sandwich, original source videos, and reconstructions from HEVC (errors magnified 10x in the bottom-right). Note the rate reduction in the sandwich result. We were not able to observe perceptually meaningful differences despite larger absolute errors.

substantially detailed output of the sandwich in places where the standard HEVC LR produces blurred results.

Perceptual Similarity Metric - LPIPS. Finally, we train sandwich HEVC YUV 4:4:4 with LPIPS using a TensorFlow implementation of [28] and compare it with the standard HEVC YUV 4:4:4 under LPIPS. The results are provided in Figures 6 and 7. Notice that the sandwich model provides $\sim 30\%$ improvements in rate over the standard HEVC across a broad range. Viewing the decoded video we observed consistent reductions in rate obtained by the sandwich system with visually imperceptible differences (e.g., Figure 6.)
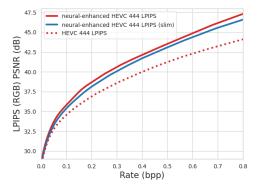

Fig. 7. RD performance of the HEVC YUV 4:4:4 sandwich trained and tested with LPIPS. Neural-enhanced HEVC YUV 4:4:4 performs $\sim 30\%$ better than the standard HEVC over a broad range of rates.

4. CONCLUSION

In this work, we extend the sandwich architecture to video compression by carefully designing a video codec proxy and training it with neural pre- and post-processors in an end-to-end fashion. The proposed sandwich model outperforms the standard codec HEVC under various settings, including YUV 4:0:0 and YUV 4:4:4 LR formats; and under ℓ_2 and LPIPS distortion, with gains of 8 dB (4:0:0), 6.5 dB (4:4:4 LR), and $\sim 30\%$ improvements in rate (LPIPS), respectively. We show that slim, light-weight networks with 57K parameters can be used to closely approximate these results. The sandwich system can not only achieve a rate-distortion performance that is substantially superior to the standard video codec but it can do so without compromising computational efficiency through the use of light-weight networks. Our results clearly demonstrate that the sandwich system can re-purpose a standard codec to compression scenarios outside its immediate scope of design, from seamlessly increasing its resolution to optimizing it for a leading perceptual quality metric, all with significant improvements.

5. REFERENCES

[1] Johannes Ballé, Valero Laparra, and Eero P Simoncelli, "End-to-end optimization of nonlinear transform codes for perceptual quality," in *2016 Picture Coding Symposium (PCS)*. IEEE, 2016, pp. 1–5.

[2] Gary J Sullivan, Jens-Rainer Ohm, Woo-Jin Han, and Thomas Wiegand, "Overview of the high efficiency video coding (hevc) standard," *IEEE Transactions on circuits and systems for video technology*, vol. 22, no. 12, pp. 1649–1668, 2012.

[3] Johannes Ballé, Philip A Chou, David Minnen, Saurabh Singh, Nick Johnston, Eirikur Agustsson, Sung Jin Hwang, and George Toderici, "Nonlinear transform coding," *IEEE Journal of Selected Topics in Signal Processing*, vol. 15, no. 2, pp. 339–353, 2020.

[4] Oren Rippel, Sanjay Nair, Carissa Lew, Steve Branson, Alexander G Anderson, and Lubomir Bourdev, "Learned video compression," in *Proceedings of the IEEE/CVF International Conference on Computer Vision*, 2019, pp. 3454–3463.

[5] Eirikur Agustsson, David Minnen, Nick Johnston, Johannes Balle, Sung Jin Hwang, and George Toderici, "Scale-space flow for end-to-end optimized video compression," in *Proceedings of the IEEE/CVF Conference on Computer Vision and Pattern Recognition*, 2020, pp. 8503–8512.

[6] Zhihao Hu, Guo Lu, and Dong Xu, "Fvc: A new framework towards deep video compression in feature space," in *Proceedings of the IEEE/CVF Conference on Computer Vision and Pattern Recognition*, 2021, pp. 1502–1511.

[7] Oren Rippel, Alexander G Anderson, Kedar Tatwawadi, Sanjay Nair, Craig Lytle, and Lubomir Bourdev, "Elf-vc: Efficient learned flexible-rate video coding," in *Proceedings of the IEEE/CVF International Conference on Computer Vision*, 2021, pp. 14479–14488.

[8] Ruihan Yang, Yibo Yang, Joseph Marino, and Stephan Mandt, "Hierarchical autoregressive modeling for neural video compression," *arXiv preprint arXiv:2010.10258*, 2020.

[9] Guo Lu, Wanli Ouyang, Dong Xu, Xiaoyun Zhang, Chunlei Cai, and Zhiyong Gao, "Dvc: An end-to-end deep video compression framework," in *2019 IEEE/CVF Conference on Computer Vision and Pattern Recognition (CVPR)*, 2019, pp. 10998–11007.

[10] Onur G Guleryuz, Philip A Chou, Hugues Hoppe, Danhang Tang, Ruofei Du, Philip Davidson, and Sean Fanello, "Sandwiched image compression: Wrapping neural networks around a standard codec," in *2021 IEEE International Conference on Image Processing (ICIP)*. IEEE, 2021, pp. 3757–3761.

[11] Onur G. Guleryuz, Philip A. Chou, Hugues Hoppe, Danhang Tang, Ruofei Du, Philip Davidson, and Sean Fanello, "Sandwiched image compression: Increasing the resolution and dynamic range of standard codecs," in *2022 Picture Coding Symposium (PCS)*, 2022, pp. 175–179.

[12] Johannes Ballé, David Minnen, Saurabh Singh, Sung Jin Hwang, and Nick Johnston, "Variational image compression with a scale hyperprior," *arXiv preprint arXiv:1802.01436*, 2018.

[13] Yueyu Hu, Wenhan Yang, Zhan Ma, and Jiaying Liu, "Learning end-to-end lossy image compression: A benchmark," *IEEE Transactions on Pattern Analysis and Machine Intelligence*, 2021.

[14] George Toderici, Damien Vincent, Nick Johnston, Sung Jin Hwang, David Minnen, Joel Shor, and Michele Covell, "Full resolution image compression with recurrent neural networks," in *Proceedings of the IEEE conference on Computer Vision and Pattern Recognition*, 2017, pp. 5306–5314.

[15] PN Tudor, "Mpeg-2 video compression," *Electronics & communication engineering journal*, vol. 7, no. 6, pp. 257–264, 1995.

[16] Vivienne Sze, Madhukar Budagavi, and Gary J Sullivan, "High efficiency video coding (hevc)," in *Integrated circuit and systems, algorithms and architectures*, vol. 39, p. 40. Springer, 2014.

[17] Gary J Sullivan, Pankaj N Topiwala, and Ajay Luthra, "The h. 264/avc advanced video coding standard: Overview and introduction to the fidelity range extensions," *Applications of Digital Image Processing XXVII*, vol. 5558, pp. 454–474, 2004.

[18] Jiaqi Zhang, Chuanmin Jia, Meng Lei, Shanshe Wang, Siwei Ma, and Wen Gao, "Recent development of avs video coding standard: Avs3," in *2019 picture coding symposium (PCS)*. IEEE, 2019, pp. 1–5.

[19] Debargha Mukherjee, Jim Bankoski, Adrian Grange, Jingning Han, John Koleszar, Paul Wilkins, Yaowu Xu, and Ronald Bultje, "The latest open-source video codec vp9-an overview and preliminary results," in *2013 Picture Coding Symposium (PCS)*. IEEE, 2013, pp. 390–393.

[20] Jingning Han, Bohan Li, Debargha Mukherjee, Ching-Han Chiang, Adrian Grange, Cheng Chen, Hui Su, Sarah Parker, Sai Deng, Urvang Joshi, et al., "A technical overview of av1," *Proceedings of the IEEE*, vol. 109, no. 9, pp. 1435–1462, 2021.

[21] P. Eusébio, J. Ascenso, and F. Pereira, "Optimizing an Image Coding Framework With Deep Learning-Based Pre- and Post-Processing," in *European Signal Processing Conf. (EUSIPCO)*, 2021, pp. 506–510.

[22] K. Qiu, L. Yu, and D. Li, "Codec-Simulation Network for Joint Optimization of Video Coding With Pre- and Post-Processing," *IEEE Open J. Circuits and Systems*, vol. 2, pp. 648–659, 2021.

[23] Y. Andreopoulos, "Neural Pre and Post-Processing for Video Encoding With AVC, VP9, and AV1," in *AOM Research Symp*, 2022.

[24] Suresh K Lodha, Alex Pang, Robert E Sheehan, and Craig M Wittenbrink, "Uflow: Visualizing uncertainty in fluid flow," in *Proceedings of Seventh Annual IEEE Visualization'96*. IEEE, 1996, pp. 249–254.

[25] O. Ronneberger, P. Fischer, and T. Brox, "U-Net: Convolutional Networks for Biomedical Image Segmentation," in *Medical Image Computing and Computer-Assisted Intervention - MICCAI 2015*, Cham, 2015, pp. 234–241.

[26] Amir Said, Manish Kumar Singh, and Reza Pourreza, "Differentiable bit-rate estimation for neural-based video codec enhancement," in *2022 Picture Coding Symposium (PCS)*, 2022, pp. 379–383.

[27] "Aom common test conditions v2.0," `http://aomedia.org/docs/CWG-B075o_AV2_CTC_v2.pdf`, Accessed: 2022-07-11.

[28] Richard Zhang, Phillip Isola, Alexei A Efros, Eli Shechtman, and Oliver Wang, "The unreasonable effectiveness of deep features as a perceptual metric," in *Proceedings of the IEEE conference on computer vision and pattern recognition*, 2018, pp. 586–595.